PIEZOELECTRIC MEMS ENERGY HARVESTERS OF PZT THIN FILMS ON STAINLESS STEEL CANTILEVERS

Y. Tsujiura, K. Adachi and I. Kanno
Mechanical engineering, Kobe University, Kobe, Japan

Abstract: We fabricated piezoelectric MEMS energy harvesters (EHs) of $Pb(Zr,Ti)O_3$ (PZT) thin films on the microfabricated stainless steel cantilevers. The 2.5-μm-thick PZT thin films were directly deposited by RF-magnetron sputtering. Direct deposition of the PZT films on the microfabricated cantilevers simplified the fabrication process of the EHs. Because of strong fracture toughness of stainless steel, the thickness of the cantilevers could be as thin as 30 μm. We obtained large averaged output power of 6.0 μW at 367 Hz and 10 m/s^2 for the unimorph cantilever (7.5 mm-long, 5.0 mm-wide) with the tip mass of 25 mg.

Keywords: energy harvesting, piezoelectric, vibration, thin film

INTRODUCTION

In recent years, there have been a lot of studies about energy harvesters (EHs) of piezoelectric thin films and it is expected to work for power sources of small electronic devices such as autonomous wireless sensor nodes [1-3]. By using EHs, it is possible to achieve the long life and maintenance-free power source instead of primary batteries. Although the power consumption of the small electronic devices decreases to tens to hundreds of μW [4], power generation of EHs is still not enough.

Vibration generators are broadly classified into three types: electromagnetic, electrostatic, and piezoelectric systems [4]. In these power generation types, piezoelectric harvesters have the simplest structure and the highest power density [1]. Furthermore, piezoelectric thin films are compatible with microelectromechanical systems (MEMS) process [4]. Therefore, it is advantageous for piezoelectric EHs to be integrated into microdevices. Piezoelectric MEMS EHs usually have the structure of unimorph cantilevers of $Pb(Zr,Ti)O_3$ (PZT) thin films on the Si substrates [5]. However, one of the problems is the fracture toughness of the cantilevers at a resonance because PZT/Si unimorph cantilevers are brittle materials. Furthermore, conventional MEMS EHs have a higher resonant frequency of more than 1 kHz, although the frequency of environmental vibrations is less than 200 Hz [4].

In this study, we fabricated the piezoelectric MEMS EHs using a metal substrate to enhance fracture toughness. In addition, a low resonant frequency can be achieved by thin metal cantilever with large tip mass. Stainless steel is relatively easy to fabricate using maicrofabrication techniques, and direct deposition of the PZT thin films on the maicroabricated stainless steel enables simple fabrication process and reduction of production cost. In this paper, we describe the fabrication and evaluation of the piezoelectric MEMS EHs of the PZT thin films deposited on the stainless steel cantilevers.

DEVICE FABRICATION

We fabricated the piezoelectric MEMS EHs of the PZT thin films deposited on the ferritic stainless steel (430) cantilevers using RF-magnetron sputtering. The coefficient of thermal expansion (CTE) of ferritic stainless steel (430) and PZT thin films are reported to be about 12×10^{-6} K^{-1} and 9×10^{-6} K^{-1}, respectively [6,7]. Small thermal stress is expected to mitigate the initial bending of the unimorph cantilevers.

Fig. 1 shows the fabrication process of the piezoelectric MEMS EHs. 30-μm-thick stainless steel cantilevers with the tip mass were fabricated from the 300-μm-thick stainless steel plate by two-step spray etching process of ferric chloride solution. As shown in Fig. 1 (1.a)~(1.c), the two-step spray etching techniques fabricates the fixed end and the tip mass of cantilevers before the PZT deposition, therefore, the fabrication process of the piezoelectric EHs can be drastically simplified. We fabricated three types of stainless steel cantilevers listed in Table 1. After deposition of Pt/Ti bottom electrodes and $(Pb,La)TiO_3$ (PLT) seed layer on the stainless steel cantilevers, the PZT thin films with a composition of Zr/Ti=53/47 were deposited by RF-magnetron sputtering [8]. The substrate was heated to around 600 °C, and deposition was performed under a mixed gas atmosphere of Ar/O_2 with a flow of 9.0/1.0 sccm. The thickness of the PZT films was 2.5 μm. The Pt top electrodes were prepared through a shadow mask. Fig. 2 shows optical images of the piezoelectric EHs of the PZT thin films on the stainless steel cantilevers.

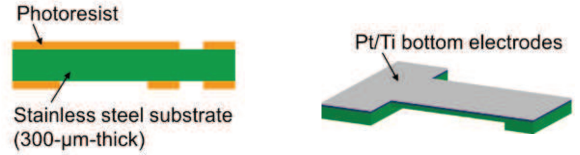

(1.a) Two-step spray etching of ferric chloride solution

(3) Pt/Ti bottom electrodes deposition

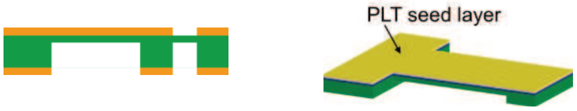

(1.b) First step of spray etching

(4) PLT seed layer deposition

(1.c) Second step of spray etching

(5) Piezoelectric PZT thin film deposition

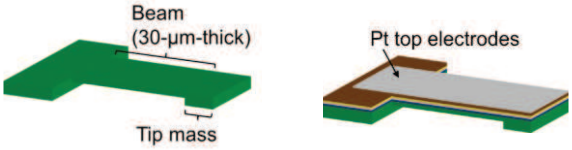

(2) Stainless steel cantilever with a tip mass

(6) Pt top electrodes deposition

Figure 1: Fabrication process of the piezoelectric PZT MEMS EHs.

CHARACTERISTICS OF PZT THIN FILMS

We evaluated the crystal structure of the PZT thin films using X-ray diffraction (XRD) techniques. Fig. 3 shows XRD patterns of the PZT thin films on the stainless steel cantilevers. Diffractions of the perovskite PZT were clearly observed, indicating pyrochlore-free PZT thin films were prepared on the Pt/Ti-coated stainless steel (430) cantilevers.

Then, we measured the dielectric properties of PZT films using an LCR meter. The relative dielectric constant ε_r and dielectric loss tanδ of the PZT films were 325~445 and 2.1~3.3 %, respectively. Although the relative dielectric constant of PZT films on the Si substrate is reported to be about 1000, low relative dielectric constant of the PZT films on stainless steel is preferable to increase the electro mechanical coupling factor k_{31} of PZT films.

Table 1: Comparison of three types of devices.

Device		Design 1	Design 2	Design 3
Dimensions (mm^2)		7.5×5.0	7.5×2.0	7.5×1.0
Tip mass (mg)		25	9.9	5.0
Peak output voltage (V)		1.1	1.1	1.6
Resonant frequency (Hz)		367	286	170
Optimum load (kΩ)		10	41	155
Maximum output power (µW)		6.0	1.7	0.9
Power density	(µW/cm^2)	16	11.3	12
	(mW/cm^3)	1.5	1.1	1.1

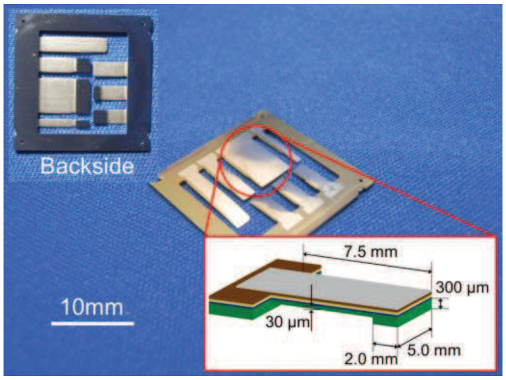

Figure 2: Photographs of the piezoelectric PZT MEMS EHs.

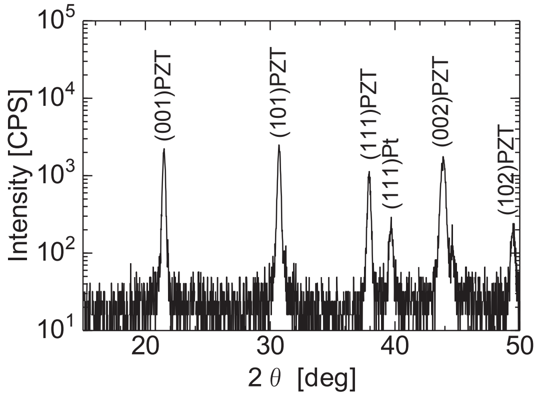

Figure 3: XRD patterns of the PZT thin films on stainless steel.

The transverse piezoelectric properties of PZT films were evaluated from the inverse piezoelectric effect of the unimorph cantilevers [9]. We applied the sinusoidal voltage at a frequency sufficiently lower than the bottom electrodes, and measured the displacement of the cantilever by laser Doppler vibrometer. The laser beam was shined at the position of 4.0 mm from the fixed end of the unimorph cantilever (7.5 mm-long, 5.0 mm-wide). From the relation between measured displacement and applied

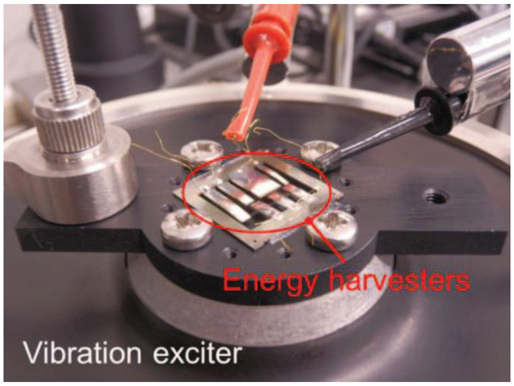

Figure 4: Measurement set-up for vibration EHs.

voltage, the transverse piezoelectric coefficient $e_{31,f}$ was calculated using Eq. (1) [9],

$$e_{31,f} = -\frac{h_s^{\,2} E_s}{3(1-\nu_s)L^2}\frac{\delta}{V} \tag{1}$$

where h_s, E_s, ν_s are the thickness, Young's modulus and Poisson's ratio of ferritic stainless steel (430), respectively. L, V, δ are the distance from the fixed end of the cantilever, applied voltage and displacement of the cantilever, respectively. From Eq. (1), the transverse piezoelectric coefficient $e_{31,f}$ was calculated to be about -4.0 C/m^2. The other unimorph cantilevers showed the almost the same $e_{31,f}$ of -4.0 C/m^2, and which is the comparable value to the transverse piezoelectric coefficient of the random-oriented PZT thin films on Si substrates [10].

POWER GENERATION

Fig. 4 shows the picture of the measurement set-up for vibration EHs. The EHs were mounted on the vibration exciter and the acceleration pickup was attached to the base of the cantilevers for monitoring the acceleration amplitude. The top and bottom electrodes of the PZT thin films were connected to a load resistance and the generated voltage was measured by an oscilloscope. We evaluated the power generation performance of PZT thin films on the stainless steel unimorph cantilevers.

Fig. 5 shows the frequency response of output voltage for design 1 in Table 1. We ramped up and down the excitation frequency and measured the output voltage with open circuit state at 10 m/s^2. A clear peak of the output voltage appeared at a resonant frequency of 367 Hz. As shown in Fig. 5, the nonlinear response was clearly observed around the resonant frequency. The nonlinear resonance, that was due to the softening spring effects, is preferable to expand the range of resonant frequency.

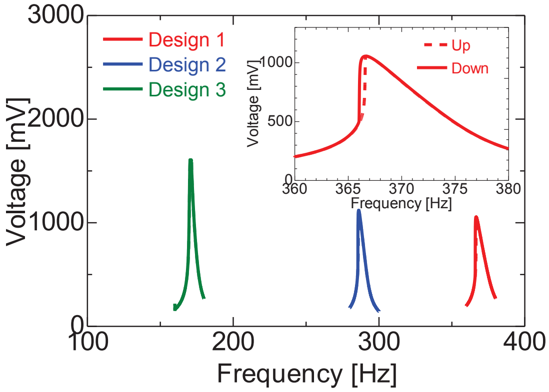

Figure 5: Output voltage of PZT EHs as a function of frequency at 10 m/s^2.

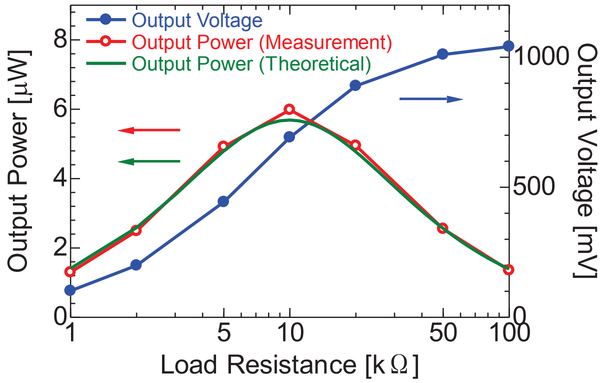

Figure 6: Output power and output voltage of PZT EH (design 1) as a function of load resistance at a resonant frequency and 10 m/s^2.

Fig. 6 shows the output power and the output voltage as a function of load resistance at 367 Hz and 10 m/s^2. The averaged output power [$P=V^2/2R$] reached 6.0 µW at the optimum load of 10 kΩ. Considering the maximum output power and the volume of the unimorph cantilever, the power density was calculated to be 1.5 mW/cm^3. We measured the other unimorph cantilevers and the results are shown in Table 1. The theoretical values of output power were calculated using Eq. (2) derived from the theoretical circuit modeling [2],

$$P = \frac{m\mu_1^{\,2}a^2}{2\omega_0}\frac{K^2\psi Q^2}{\psi^2+\left(1+K^2\psi Q\right)^2} \tag{2}$$

$$\psi = \omega_0 RC \tag{3}$$

where m, μ_1, a, ω_0, K, Q are equivalent mass, correction factor which is determined by the ratio of the tip mass to the beam mass, acceleration amplitude, fundamental mechanical angular frequency, generalized electro mechanical coupling factor (GEMC) and quality factor, respectively. R and C are load resistance and the capacitance of cantilever, respectively. GEMC (K^2) indicates the conversion efficiency between the electric and vibration energy in

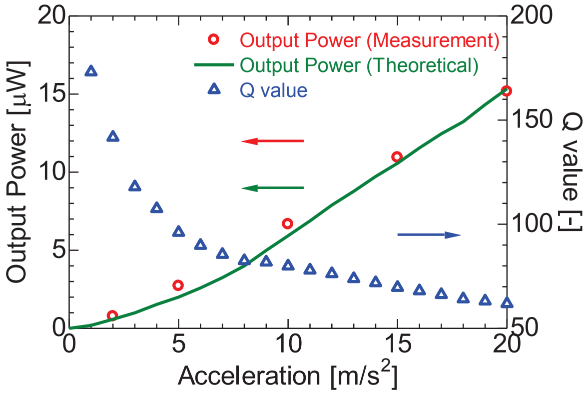

Figure 7: Output power and Q value of PZT EH (design 1) as a function of acceleration at a resonant frequency and an optimum load.

piezoelectric materials. In this study, we evaluated K^2 by comparison of output power between measured and theoretical values of Eq. (2). K^2 of the PZT films on the stainless steel cantilever was calculated to be 4.4×10^{-3}, and almost the same values were obtained for the other stainless steel cantilevers. Compared to K^2 of the PZT films on the Si cantilever (2.2×10^{-4}) [2], we achieved an extremely high conversion efficiency for PZT EHs of the stainless steel cantilevers.

Fig. 7 shows the output power and Q value as a function of acceleration. The optimum output power was measured at the accelerations ranging from 1 to 20 m/s^2 under the conditions of 367 Hz and 10 kΩ; besides, the theoretical output power was calculated from Eq. (2). From Fig. 7, the measured values were in good agreement with the theoretical values. Furthermore, the output power reached 15 μW under the acceleration of 20 m/s^2 without the destruction of cantilever. We obtained the Q value by using the half-power bandwidth method and confirmed that the *Q* value rapidly decreased as the acceleration increased as shown in Fig. 7. This is because the air damping increased with the acceleration. Another reason is that larger displacements of the cantilever enhanced the nonlinearity and then expanded the bandwidth.

CONCLUSION

We fabricated the piezoelectric MEMS EHs of microfabricated stainless steel cantilevers. The stainless steel cantilevers with built-in tip mass were fabricated by using a two-step spray etching process. PZT thin films had a polycrystalline perovskite structure and showed the low relative dielectric constant (ε_r: 325~445) with low dielectric loss (tanδ: 2.1~3.3 %). The transverse piezoelectric coefficient $e_{31,f}$ was about -4.0 C/m^2. From the evaluation of power generation performance of unimorph cantilever (7.5 mm-long, 5.0 mm-wide) with the tip mass of 25 mg, maximum output power was 6.0 μW under conditions of 367 Hz, 10 kΩ and 10 m/s^2. The K^2 of the PZT films on stainless steel determined by fitting theoretical values to experimental values was 4.4×10^{-3}. Our PZT MEMS EHs showed the nonlinear resonance of the softening spring effects, therefore, relatively wide bandwidth EHs were achieved.

REFERENCES

[1] S. Roundy and P. K. Wright, A piezoelectric vibration based generator for wireless electronics, *Smart Mater. Struct.* **13** (2004) 1131-1142.

[2] M. Renaud, K. Karakaya, T. Sterken, P. Fiorini, C. Van Hoof and R. Puers, Fabrication, modeling and characterization of MEMS piezoelectric vibration harvesters, *Sens. Actuators A* **145-146** (2008) 380-386.

[3] R. Andosca, T. G. McDonald, V. Genova, S. Rosenberg, J. Keating, C. Benedixen and J. Wu, Experimental and theoretical studies on MEMS piezoelectric vibrational energy harvesters with mass loading, *Sens. Actuators A* **178** (2012) 76-87.

[4] S. Roundy, P. K. Wright and J. Rabaey, A study of low level vibrations as a power source for wireless sensor nodes, *Computer Communications* **26** (2003) 1131-1144.

[5] Q.-M. Wang, X.-H. Du, B. Xu and L. E. Cross, Electromechanical Coupling and Output Efficiency of Piezoelectric Bending Actuators, *IEEE Trans. Ultrason. Ferroelect. Freq. Contr.* **46** (1999) 638-646.

[6] M. W. Hooker, Properties of PZT-based Piezoelectric Ceramics Between -150 and 250 °C, *NASA CR* (1998) 208708.

[7] X. Chen, P. Y. Hou, C. P. Jacobson, S. J. Visco and L. C. De Jonghe, Protective coating on stainless steel interconnect for SOFCs: oxidation kinetics and electrical properties, *Solid State Ionics* **176** (2005) 425-433.

[8] T. Suzuki, I. Kanno, J. J. Loverich, H. Kotera and K. Wasa, Characterization of Pb(Zr,Ti)O_3 thin films deposited on stainless steel substrates by RF-magnetron sputtering for MEMS applications, *Sens. Actuators A* **125** (2006) 382-386.

[9] I. Kanno, H. Kotera, K. Wasa, Measurement of transverse piezoelectric properties of PZT thin films, *Sens. Actuators A* **107** (2003) 68-74.

[10] P. Muralt, Recent Progress in Material Issues for Piezoelectric MEMS, *J. Am. Ceram. Soc.* **91** (2008) 1385-1396.